

CsiLAC4 modulates boron flow in *Arabidopsis* and *Citrus* via high-boron-dependent lignification of cell walls

Jing-Hao Huang^{1,2} , Ling-Yuan Zhang³, Xiong-Jie Lin¹ , Yuan Gao⁴, Jiang Zhang², Wei-Lin Huang¹, Daqiu Zhao⁵, Rhuano Soranz Ferrarezi⁶ , Guo-Cheng Fan^{1,7} and Li-Song Chen^{2,8} 

¹Pomological Institute, Fujian Academy of Agricultural Sciences, Fuzhou 350013, China; ²Institute of Plant Nutritional Physiology and Molecular Biology, College of Resources and Environment, Fujian Agriculture and Forestry University, Fuzhou 350002, China; ³Fujian University of Traditional Chinese Medicine, Fuzhou 350122, China; ⁴College of Horticulture, Fujian Agriculture and Forestry University, Fuzhou 350002, China; ⁵College of Horticulture and Plant Protection, Yangzhou University, Yangzhou 225009, China; ⁶Department of Horticulture, the University of Georgia, Athens, GA 30602, USA; ⁷Institute of Plant Protection, Fujian Academy of Agricultural Sciences, Fuzhou 350013, China; ⁸Fujian Provincial Key Laboratory of Soil Environmental Health and Regulation, College of Resources and Environment, Fujian Agriculture and Forestry University, Fuzhou 350002, China

Summary

Authors for correspondence:

Jing-Hao Huang

Email: jhuang1982@126.com

Guo-Cheng Fan

Email: guochengfan@126.com

Li-Song Chen

Email: lisongchen2002@hotmail.com

Received: 4 April 2021

Accepted: 3 November 2021

New Phytologist (2022) 233: 1257–1273

doi: 10.1111/nph.17861

Key words: boron toxicity, cell walls, *Citrus*, laccase-like protein, nutrient transport, nutrient uptake.

- The mechanisms underlying plant tolerance to boron (B) excess are far from fully understood. Here we characterized the role of the miR397-CsiLAC4/CsiLAC17 (from *Citrus sinensis*) module in regulation of B flow.
- Live-cell imaging techniques were used in localization studies. A tobacco transient expression system tested modulations of CsiLAC4 and CsiLAC17 by miR397. Transgenic *Arabidopsis* were generated to analyze the biological functions of CsiLAC4 and CsiLAC17. CsiLAC4's role in xylem lignification was determined by mRNA hybridization and cytochemistry. *In situ* B distribution was analyzed by laser ablation inductively coupled plasma mass spectrometry.
- CsiLAC4 and CsiLAC17 are predominantly localized in the apoplast of tobacco epidermal cells. Overexpression of *CsiLAC4* in *Arabidopsis* improves the plants' tolerance to boric acid excess by triggering high-B-dependent lignification of the vascular system's cell wall and reducing free B content in roots and shoots. In *Citrus*, *CsiLAC4* is expressed explicitly in the xylem parenchyma and is modulated by B-responsive miR397. Upregulation of *CsiLAC4* in *Citrus* results in lignification of the xylem cell walls, restricting B flow from xylem vessels to the phloem.
- CsiLAC4 contributes to plant tolerance to boric acid excess via high-B-dependent lignification of cell walls, which set up a 'physical barrier' preventing B flow.

Introduction

Boron (B) is a metalloid element belonging to group 13 in the periodic table (Tu *et al.*, 2010). In aqueous solutions or soils with pH < 7, B occurs as undissociated boric acid (H₃BO₃), which can equilibrate across the phospholipid bilayers of biological membranes by permeation and penetrate cells through passive channel proteins or by secondary active efflux transporters under deficiency conditions (Raven, 1980; Takano *et al.*, 2002; Kato *et al.*, 2009; Reid, 2014). Boric acid in the cytoplasmic compartment of plant and animal cells can quickly react with a variety of hydroxyl-rich compounds (Loomis & Durst, 1992; Bolaños *et al.*, 2004).

As a micronutrient, B is required for the growth, development and reproduction of all higher vascular plants (Saleem *et al.*, 2011; Chatterjee *et al.*, 2014; Durbak *et al.*, 2014). The B concentration needed for different crops varies significantly with species and cultivars; observed B concentrations in monocots are

generally lower than in dicots (Princi *et al.*, 2016). Nevertheless, the optimal B range for plant growth and development is very narrow in particular species (Bingham *et al.*, 1987). Both deficient and excessive B levels can easily be noticed in several crops (Nable *et al.*, 1997; Shorrocks, 1997; Chen *et al.*, 2012; Landi *et al.*, 2019). B excess in soils generally results in overaccumulation of B in the aboveground plant parts due to its passive transport within the transpiration stream, thereby generating toxicity to plants (Nable *et al.*, 1990; Brdar-Jokanovic, 2020).

Plant tolerance to excessive B varies within and between species and is primarily determined by B's reallocation and/or transportation ability (Nable *et al.*, 1997; Brdar-Jokanovic, 2020). In plant species where B forms stable borates with primary photosynthetic polyols, B can be reallocated by the phloem, and the symptomatology of B excess is seldom observed in mature organs. By contrast, typical symptoms of B toxicity in phloem immobile plants are expressed in older leaf margins due to enrichment of B at the end of the transpiration stream (Brown & Shelp, 1997).

The mechanism underlying tolerance to B excess in B-immobile plants can be attributed to the efflux of B by transporters. For instance, the expression of efflux transporter BOR1 in barley (*Hordeum vulgare*) can reduce B uptake, thereby decreasing B concentration in shoots. At the same time, the expression of *BOR1* homologs in *Arabidopsis* (*Arabidopsis thaliana*) reduces B uptake by the roots and redistributes toxic B within the shoots. With this strategy, plants can reduce intracellular B levels (Hayes & Reid, 2004; Miwa *et al.*, 2007, 2014; Sutton *et al.*, 2007).

However, the efflux-based theory could not explain the fact that B tolerance was not reliably correlated with lower tissue B concentrations in many plant species (Nable *et al.*, 1990; Torun *et al.*, 2006; Ochiai *et al.*, 2011; Huang *et al.*, 2014). Within-species genotypes with similar tissue B concentrations can show remarkably different toxicity symptoms (Reid & Fitzpatrick, 2009). To explain these observations, a detoxifying mechanism exerted by B-chelating compounds such as polyols and phenolics was proposed (Princi *et al.*, 2016). Supporting evidence was found in a recent study on loquat (*Eriobotrya japonica*), which revealed an orchestrated defensive mechanism to deal with B toxicity by shifting carbohydrate metabolites from sucrose to sorbitol and fructose (Papadakis *et al.*, 2018). Yet, such a mechanism is uncommon for those species that do not use polyols as translocating agents (Landi *et al.*, 2019). Some authors speculated that B might be compartmentalized in the vacuoles or the cell walls via transporters (Reid & Fitzpatrick, 2009; Martinez-Cuenca *et al.*, 2015). However, maintenance of B distribution across membranes within cells by active transport of boric acid away from thermodynamic equilibrium is likely to be energetically expensive and inefficient, as 99.95% of B in the plant cytoplasm exists in the form of boric acid, equilibration of which occurs within minutes at high concentrations (Raven, 1980; Reid, 2014; Princi *et al.*, 2016). To date, limited information is available on vacuolar B concentrations and molecular characterization of B-complexes within vacuoles (Wimmer *et al.*, 2020). The tolerance mechanisms of plants to B excess remain to be elucidated.

Citrus (*Citrus* sp.) is one of the most important fruit crops cultivated around the globe. *Citrus* plants are sensitive to B excess, which generates toxicity to old mature leaves (Han *et al.*, 2009; Chen *et al.*, 2012). B toxicity to *Citrus* mainly occurs in B-rich soils or in soils where B fertilizers are applied inappropriately and has been reported worldwide, resulting in an overall reduction in tree vigor and yield (Nable *et al.*, 1997; Papadakis *et al.*, 2004; Huang *et al.*, 2014; Li *et al.*, 2015; Martinez-Cuenca *et al.*, 2015). As reported for many other species, variation in high B tolerance appeared in different genotypes of *Citrus*. Studies have shown that the tolerance mechanism of *Citrus* to B excess is independent of B efflux (Sheng *et al.*, 2010) and that B-chelating organic compounds made almost no contribution to detoxification under boric acid-toxic stress (Martinez-Cuenca *et al.*, 2015). These studies implied a novel B tolerance mechanism in plants.

Citrus sinensis (B-tolerant) and *Citrus grandis* (B-intolerant) are two *Citrus* plants showing different tolerance to B excess. However, they maintain a similar total B content in the leaves under excessive B conditions (Guo *et al.*, 2014). Previously, we found that excessive boric acid treatment triggers explicitly programmed

cell death of the phloem tissue in intolerant *C. grandis*, and that miR397 plays a role in this process via targeting *LAC4* and *LAC17*, both belonging to the laccase family (Huang *et al.*, 2014, 2016). Laccases are enzymes that can oxidize quinol. They are involved in protoplast regeneration, and lignification and delignification of plant cell walls (Mayer & Staples, 2002; Schuetz *et al.*, 2014). In *Arabidopsis*, *LAC4* and *LAC17* contribute to the constitutive lignification of stems, while *LAC17* is involved in the deposition of guaiacyl lignin units in fibers (Berthet *et al.*, 2011). In the present study, through detailed functional analysis of *Csi-miR397* and its targets, *CsiLAC4* and *CsiLAC17* in *Arabidopsis* and *Citrus*, we reveal a distinct B tolerance mechanism in *Citrus*. We show that *CsiLAC4*, targeted by miR397, modulates secondary lignification of the xylem parenchyma cell walls, which limits B inflow to the phloem to alleviate toxicity in B-tolerant *C. sinensis*. Interestingly, the functioning of *CsiLAC4* in cell wall lignification is high-B dependent.

Materials and Methods

Plant materials and growth conditions

Five-week-old seedlings of 'Xuegan' sweet orange (*C. sinensis*, tolerant to B excess) and sour pummelo (*C. grandis*, intolerant to B excess) were cultured and treated with sufficient (10 μM , control) and excessive boric acid (400 μM) for 15 wk as previously reported by Huang *et al.* (2014) in a glasshouse under natural photoperiod. Mature leaves were sampled at one-third height (*c.* 30 cm above ground) of the seedlings and used for total RNA extraction, cell wall extraction, histochemical analysis, *in vitro* hybridization and *in situ* B distribution analysis.

The transgenic and wild-type *Arabidopsis* (*A. thaliana*, Col-0) seeds were sterilized for 15 min in 1.5% bleach and then rinsed five times with double-distilled water. Sterilized seeds were kept at 4°C for 3 d before being grown on ½ Murashige & Skoog (½MS) agar-medium (pH 5.8). Plants were cultivated in vertical chambers with a light intensity of 222 $\mu\text{mol m}^{-2} \text{s}^{-1}$ and 16 h : 8 h (day : night) photoperiod. Tobacco (*Nicotiana benthamiana*) and *Arabidopsis* seedlings were transplanted in 10 × 10 × 10 cm plastic pots containing peat moss and vermiculite (2 : 1, v/v) and grown in chambers under the same light conditions with a constant relative humidity of 45%. B in peat moss and vermiculite was leached away with 0.1 M HCl. The HCl-treated medium was thoroughly washed with distilled water and dried before use.

Total RNA extraction and cDNA synthesis

Total RNAs were extracted from boric acid-treated *Citrus* and *Arabidopsis* samples or tobacco leaves with TRIzol reagent (Invitrogen). The quantity and purity of the total RNAs were determined with a NanoDrop 2000 spectrophotometer (Thermo Scientific, Waltham, MA, USA) and a 2100 bioanalyzer (Agilent, Santa Clara, CA, USA). Total RNAs with RNA integrity number > 8.0 were converted into cDNA using a Maxima First Strand cDNA Synthesis Kit (Thermo Scientific) when indicated.

Cloning of *pre-miR397*, *CsiLAC4* and *CsiLAC17*, and vector construction

For cloning of *pre-miR397*, the predicted precursor of miR397 was aligned to the Orange Genomic Database (<http://citrus.hzau.edu.cn/orange>) (Huang *et al.*, 2016). A genomic DNA sequence containing the precursor and ± 500 bp down- and upstream was subjected to primer search. Primers were designed *c.* 300 bp up- and downstream from the precursor, and the expected PCR product should not change the secondary structure of the contained precursor (ViennaRNA Web Services; <http://rna.tbi.univie.ac.at>). The *pre-miR397* fragments were amplified from *C. sinensis* DNA with the primers listed in Supporting Information Table S1.

The sequences of *CsiLAC4* (Cs6g07800.1) and *CsiLAC17* (Cs8g17630.1) were obtained from the *C. sinensis* genome (<http://citrus.hzau.edu.cn/orange/index.php>). The open reading frames (ORFs) of *CsiLAC4* and *CsiLAC17* were cloned by high-fidelity PCR amplification from *C. sinensis* cDNA. The primers are listed in Table S1.

PCR products were gel-purified. For overexpression, recovered fragments were double-digested with *Bam*HI and *Sac*I (for overexpression) and ligated overnight with T4 DNA ligase (New England Biolabs (NEB), Ipswich, MA, USA) to the pretreated pBI121 vector (Fig. S1). For DsRed-fused expressions, recovered fragments were directly ligated to the *Xba*I/*Bam*HI-predigested pBI121-DsRed vector using an In-Fusion[®] HD Cloning Kit (Takara Bio, Shiga, Japan). Confirmed constructs overexpressing DsRed-fused *CsiLAC4* or *CsiLAC17* were mutated with a Hieff Mut[™] Site-directed Mutagenesis Kit (Yeasen, Shanghai, China) according to the manufacturer's instructions. Primers used for mutagenesis are available in Table S2. All constructs were determined by sequencing and then introduced into *Agrobacterium* GV3101 (pSoup) using the freeze–thaw method.

Bioinformatics, sequence alignment and phylogenetic analysis

For bioinformatics analysis of *CsiLAC4* and *CsiLAC17*, signal peptides and transmembrane topology were predicted using the online software POBIUS (<http://phobius.sbc.su.se/index.html>) and SOSUI (<http://harrier.nagahama-i-bio.ac.jp/sosui>), and multiple sequence alignments were performed in MEGA7 (Kumar *et al.*, 2016).

Subcellular localization of *CsiLAC4* and *CsiLAC17*

For subcellular localization assays, C-terminally tagged *CsiLAC4*-DsRed or *CsiLAC17*-DsRed was transiently coexpressed with the green fluorescent protein (GFP) in tobacco epidermal cells through *Agrobacterium*-mediated transfection (Agroinoculation) (Sparkes *et al.*, 2006). Coexpression of untagged DsRed and GFP was set as a control. Seventy-two hours post-transfection, leaf blades were injected with 0.8 M sorbitol before being subjected to microscopy. Fluorescence signals were examined using a DMi8 confocal laser scanning microscope (Leica, Wetzlar, Germany).

In situ mRNA hybridization

Boric acid-treated *C. sinensis* and *C. grandis* leaf samples were fixed overnight in a 1 : 1 : 18 solution of formaldehyde, acetic acid and 50% ethanol (FAA) and applied for serial paraffin sections (5 μ m) as reported by Huang *et al.* (2019b).

Gene-specific primers for *miR397*, *CsiLAC4* and *CsiLAC17* (Table S1) were used to amplify the probe templates from *C. sinensis* cDNA. PCR products were gel-purified and sequenced. Sense and complementary digoxigenin-labeled RNA probes were synthesized with a DIG RNA Labeling Kit (Roche) according to the manufacturer's instructions. *In situ* hybridization was performed on the paraffin sections as described by Braissant & Wahli (1998). Signals were visualized with a DIG Nucleic Acid Detection Kit (Roche) and photographed under a BX-41 light microscope (Olympus, Tokyo, Japan).

MicroRNA blotting

Pre-miR397 was transiently expressed in tobacco leaves via Agroinoculation (Sparkes *et al.*, 2006). Inoculation of *Agrobacterium* without any construct was set as a mock, and those with other constructs as controls. Total RNA was extracted 48 h postinoculation, and miR397 abundance was determined by microRNA blotting.

Thirty micrograms of total RNA from each sample was used for gel blot hybridization, according to Fei *et al.* (2018). DNA oligo probes (Table S3) were end-labeled with γ -³²P-ATP using T4 Polynucleotide Kinase (NEB). U6 small nuclear RNA was used as a loading control in *Citrus* and tobacco (Zhao *et al.*, 2013; Eamens *et al.*, 2014). After overnight exposure with the hybridized membrane, phosphor screens were scanned using a Typhoon scanner (GE Healthcare Bio-Sciences, Chicago, IL, USA).

Modulation of *CsiLAC4* and *CsiLAC17* by miR397

We tested the hypothesis that miR397 directly cleaves *CsiLAC4* and *CsiLAC17* mRNAs with the *Agrobacterium*-mediated delivery system in tobacco leaves as described by Llave *et al.* (2002), and the 5'-end mRNA cleavage products were detected by nested 5'-RACE (rapid amplification of cDNA ends) PCR using a Smart Race Kit (Takara Bio) according to the manufacturer's instructions. Gene-specific primers are listed in Table S4. For visualization research, the empty GFP construct was coexpressed and used as an indicator of successful transfection; coexpressions of *pre-miR397* with the mutated *CsiLAC4*-DsRed or *CsiLAC17*-DsRed construct were set as controls. Fluorescence signals were detected 48 h after inoculation under a DMi8 confocal laser scanning microscope (Leica). For each assay, the transformation was performed in three leaves from different tobacco plants.

CsiLAC4 and *CsiLAC17* functions in *Arabidopsis*

Transgenic *Arabidopsis* plants overexpressing *CsiLAC4*, *CsiLAC17* and *pre-miR397* were obtained by *Agrobacterium*-

mediated transformation using the floral dip method (Zhang *et al.*, 2006). For each gene, two transgenic lines showing a segregation ratio of 3 : 1 (resistance : susceptibility to kanamycin) were selected and grown to the homozygous T4 generation for further studies. For phenotypic analysis, vernalized Col-0 and T4 seeds were grown on ½MS agar-medium supplemented with 0, 0.5, 1, 2, 5 and 10 mM boric acid, or with 0, 10, 50, 100 and 200 mM NaCl, respectively. The shoot fresh weight and the hypocotyl and total root length were measured 14 d after sowing using WINRHIZO 2009b (Regent, Montreal, QC, Canada) as reported by Huang *et al.* (2019a). For continuous assessment of CsiLAC4 functioning in B tolerance, uniform 3-wk-old T4 seedlings grown in 1 l plastic pots (four plants per pot) were irrigated with 100 ml ½ liquid MS medium (supplemented with 0, 1, 2 and 5 mM boric acid) every other day for 2 wk. Above-ground plant parts were then dried and weighed.

Lignin content measurement

One gram of inflorescence stem or rosette leaf tissues from 5-wk-old Col-0 and T3 seedling was used for extraction of cell wall material as described by Zhong & Lauchli (1993), and then the Klason lignin content was determined according to Hatfield *et al.* (1994).

Determination of B and other mineral nutrients

Citrus leaves and *Arabidopsis* roots and shoots were used for B determination. All the samples were ground into fine powder in liquid N₂, and B fractions were extracted (soluble in water, soluble in organic solvents and insoluble) (Martinez-Cuenca *et al.*, 2015). Briefly, the powders were extracted twice with ice-cold water (10 volumes) and centrifuged at 9400 g for 10 min. Combined supernatants were used for water-soluble B (free B) determination. The residues were washed three times with 80% ethanol (10 volumes), once with a methanol : chloroform mixture (1 : 1, v/v; 10 volumes) and once with acetone (10 volumes). The combined organic extracts in which monolignols were available were used for organic-bound B determination and the pellets for cell wall-bound B. All the B fractions were freeze-dried and ashed in a muffle furnace at 550°C for 12 h.

Total B and Zn, Cu, Mn, Mg and Ca concentrations from dried rosette leaves and roots extracted from mature plants were determined by inductively coupled plasma MS (ICP-MS).

Anatomy and histochemistry

Main veins from boric acid-treated *Citrus* leaves and hypocotyl and root segments from 14-d-old boric acid-treated *Arabidopsis* were fixed in FAA for 24 h. Tissue samples were then subjected to routine serial paraffin sectioning (5 µm). Transverse sections were deparaffinized, stained with 5% phloroglucinol in 1 M HCl for 5 min according to the Wiesner's reaction (Žárský & Cvrčková, 2019) and visualized under an Axio Imager 2 light microscope (Zeiss).

Fresh inflorescence stems from 5-wk-old boric acid-treated plants were hand-sectioned. Thin sections were stained with 5% phloroglucinol in 1 M HCl and observed under a light microscope.

Measurement of gene expression and micro-RNA assay

To monitor the expression of laccase-like family genes in response to boric acid excess, *Citrus* leaves and *Arabidopsis* shoots and roots were treated with boric acid. Real-time (RT) PCRs were set up with 2× SYBR Green qPCR Master Mix (Takara Bio). Amplification levels were detected with a CFX96 Touch RT-PCR Detection System (Bio-Rad). Quantification was performed using three independent biological replicates. *β-actin* and *tubulin* were set as internal controls for *Citrus* and *GAPDH* and *UBQ5* (Joseph *et al.*, 2018) for *Arabidopsis*. To monitor the relative abundance of miR397 in *Arabidopsis* treated with different levels of boric acid, stem-loop RT-PCR was conducted with a TaqMan[®] MicroRNA Assay Kit (Takara Bio) as previously described (Huang *et al.*, 2016). All the primers employed for RT-PCR are listed in Table S5. Relative levels were expressed as 2^{-ΔΔC_t}. Heatmaps were generated using EXCEL 2016 (Microsoft, Redmond, WA, USA).

Laser ablation (LA) ICP-MS analysis

For *in situ* B distribution, fresh main-veins of boric acid-treated *Citrus* leaves were transversely sectioned (24 µm) with an MEV freezing microtome (Slee Medical, Mainz, Germany). Cryosections were mounted on poly-L-lysine-coated glass slides and then freeze-dried at -40°C immediately to minimize B diffusion. Prepared slides were photographed with a light microscope before being applied to GeoLasPro LA-ICP-MS (Coherent, Santa Clara, CA, USA). Laser ablation was performed in line scanning mode with carrier helium gas flow of 600 ml min⁻¹, laser power set to 20% and laser spot diameter of 20 µm. The 7500a ICP-MS (Agilent) was set up in time-resolved analysis mode, and the resulting amounts of B were reported in counts per second. Finally, a B distribution contour was generated from the ICP-MS data that represents the total count of the B signal at each time point using ORIGINPRO 9.0 (Origin Lab, Northampton, MA, USA).

Quantification and statistical analysis

Boron content, shoot fresh weight, total root length and hypocotyl length of transgenic *Arabidopsis* treated with different B levels were analyzed using two-way between-group ANOVA followed by Sidak's *post-hoc* test in SPSS 22.0 (IBM, Armonk, NY, USA). An independent *t*-test was used to determine the statistical significance between samples in assays related to lignin or B contents. Bivariate correlation analysis was performed to examine the correlation between relative expressions of genes in transgenic lines and the external B levels. Statistic results were presented by SIGMAPLOT 10.0 (Systat, Palo Alto, CA, USA) and EXCEL 2016 (Microsoft).

Results

miR397 mediates cleavage of *CsiLAC4* and *CsiLAC17* mRNAs

For validation of miR397 targeting *CsiLAC4* and *CsiLAC17*, we used the tobacco transient expression system. We inoculated tobacco leaves with different combinations of *Agrobacterium* strains, which respectively carry the *pre-miR397*, DsRed-fused *CsiLAC4* and *CsiLAC17* constructs. Based on micro-RNA (miRNA) blotting, we showed that heterologously expressing *pre-miR397* in tobacco efficiently generated mature miR397 (Fig. 1a). We then detected miRNA-mediated decay of *CsiLAC4* and *CsiLAC17* mRNA using 5'-RACE PCR. We only obtained a full-length 5'-end fragment from the nested PCR when the *CsiLAC4* or *CsiLAC17* construct was

inoculated alone. Besides the corresponding full-length 5'-ends, we obtained the expected cleavage product for each target (718 bp for *CsiLAC4* and 217 bp for *CsiLAC17*) when cotransfection was performed. Unexpectedly, we also acquired another 670 bp fragment from tobacco leaves coinoculated with the *CsiLAC17* and *pre-miR397* constructs (Fig. 1b). Under the confocal microscope, the DsRed-fused *CsiLAC4* and *CsiLAC17* fluorescent signals that should have appeared in the epidermal cells were suppressed when *pre-miR397* was coinoculated. Interestingly, an introduction of several site-directed mutations in the miR397 complementary sites of *CsiLAC4*-*DsRed* or *CsiLAC17*-*DsRed* mRNA led to the recovery of the DsRed fluorescent signals (Fig. 1c,d). These results provided solid evidence that *CsiLAC4* and *CsiLAC17* are posttranscriptionally regulated through miR397-mediated cleavage of the corresponding mRNAs.

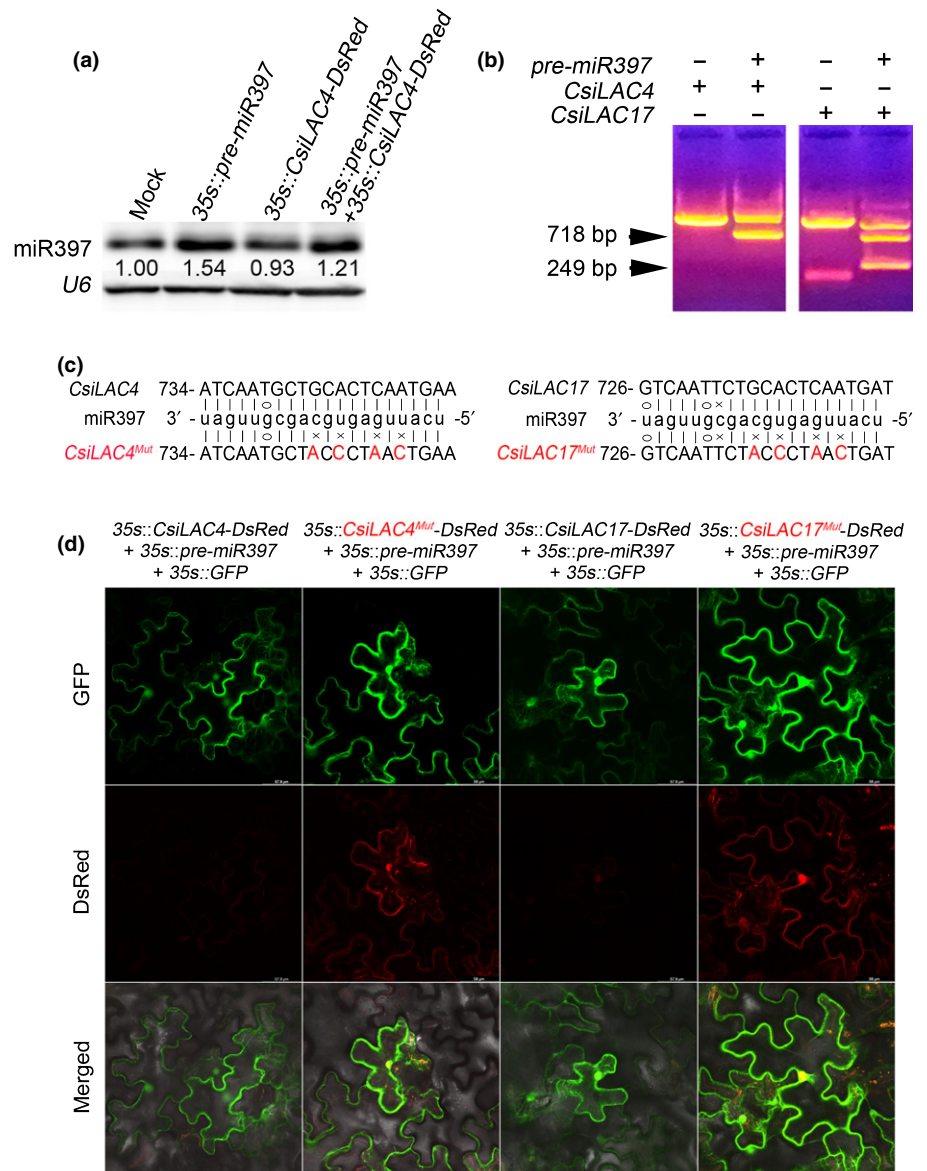


Fig. 1 miR397 modulates expression of fluorescently tagged *CsiLAC4* and *CsiLAC17* in tobacco leaf via miRNA-mediated cleavage of mRNA. (a) miRNA blot showing generation of mature miR397 by transient expression of *pre-miR397* in tobacco leaves. Total RNAs were extracted 48 h postinoculation. (b) 5'-RACE PCR of *CsiLAC4* and *CsiLAC17* from tobacco leaves coexpressing miR397 and *CsiLAC4*-*DsRed*/*CsiLAC17*-*DsRed*. Arrowheads indicate expected fragments supporting the miRNA-mediated cleavage. (c) Site-directed mutations of *CsiLAC4* and *CsiLAC17* in complementary sites of miR397. Mutated nucleotides are indicated in red. (d) miR397 represses expression of DsRed-tagged *CsiLAC4* and *CsiLAC17* rather than their corresponding mutants in the tobacco epidermis. Confocal micrographs were obtained 48 h posttransfection. GFP was used as an indicator of successful transfection.

Bioinformatics and subcellular localization of CsiLAC4 and CsiLAC17

CsiLAC4 and CsiLAC17 share 77.10% and 78.56% identity with *Arabidopsis* laccase-4 and laccase-17, respectively (Fig. S2). Both proteins were predicted in the cell membrane (PLANT-MPLOC; <http://www.csbio.sjtu.edu.cn/bioinf/plant-multi>). However, topology analysis (PHOBIUS; <http://phobius.sbc.su.se/index.html>) revealed that neither CsiLAC4 nor CsiLAC17 contains the transmembrane domain and that the majority of their peptides were noncytoplasmic (Fig. S3). For subcellular localization, we fused CsiLAC4 and CsiLAC17 to the N-termini of the DsRed reporter and coexpressed them with GFP in tobacco epidermal cells. Plasmolysis of epidermal cells showed that CsiLAC4 was predominantly localized in the apoplast and CsiLAC17 in the cell walls and protoplast (Fig. S4).

A gene search of the NCBI database showed several homologs of CsiLAC4 and CsiLAC17 from other plant and animal species. According to the phylogenetic analysis, CsiLAC4 homologs, but not CsiLAC17, clustered into the dicot group, which markedly could be clustered into five subgroups by herbaceous and woody types (Figs 2, S5). This implied that the laccase-4 homologs in woody species might function differently from those in herbaceous species.

Overexpression of CsiLAC4 in *Arabidopsis* increases plant tolerance to B excess

Overexpression of *AtLAC4* or *AtLAC17* in *Arabidopsis* causes ectopic lignification of cotyledon epidermal cell walls when exogenous monolignols are supplied (Schuetz *et al.*, 2014). To evaluate ectopic functions of *Csi-miR397*, *CsiLAC4* and *CsiLAC17* in *Arabidopsis* cell wall lignification, we created several transgenic lines overexpressing *pre-miR397* (*miR397^{OE}*), *CsiLAC4* (*CsiLAC4^{OE}*) and *CsiLAC17* (*CsiLAC17^{OE}*) from Col-0 *Arabidopsis*. Surprisingly, under moderate B conditions, no significant difference was found for Klason lignin contents of rosette leaves and inflorescence stems between the transgenic lines and Col-0. However, the lignin content of *miR397^{OE}* inflorescence stems was lower than in those of *CsiLAC4^{OE}* and *CsiLAC17^{OE}* lines (Fig. S6).

Given that *miR397*, *CsiLAC4* and *CsiLAC17* are involved in the response of *Citrus* to B toxicity (Huang *et al.*, 2016), we treated the T4 transgenic seedlings with excessive boric acid for 14 d. *CsiLAC4^{OE}* lines showed better growth performances than Col-0 plants after the boric acid treatment (Figs 3a, S7a). We determined the shoot fresh weight, total root length and hypocotyl length of each seedling, and the results showed significant reductions of shoot fresh weight and total root length in all plant lines as external boric acid increased (Fig. 3b,c). Nonetheless, the shoot fresh weight of *CsiLAC4^{OE}* lines was higher than the remaining lines under excessive B conditions (Fig. 3b), while total root length of *CsiLAC4^{OE}* lines was higher than the others when external boric acid concentrations were < 2 mM (Fig. 3c). Moreover, external boric acid for a concentration of < 5 mM increased the hypocotyl length in *CsiLAC4^{OE}* lines (Fig. S7a,b).

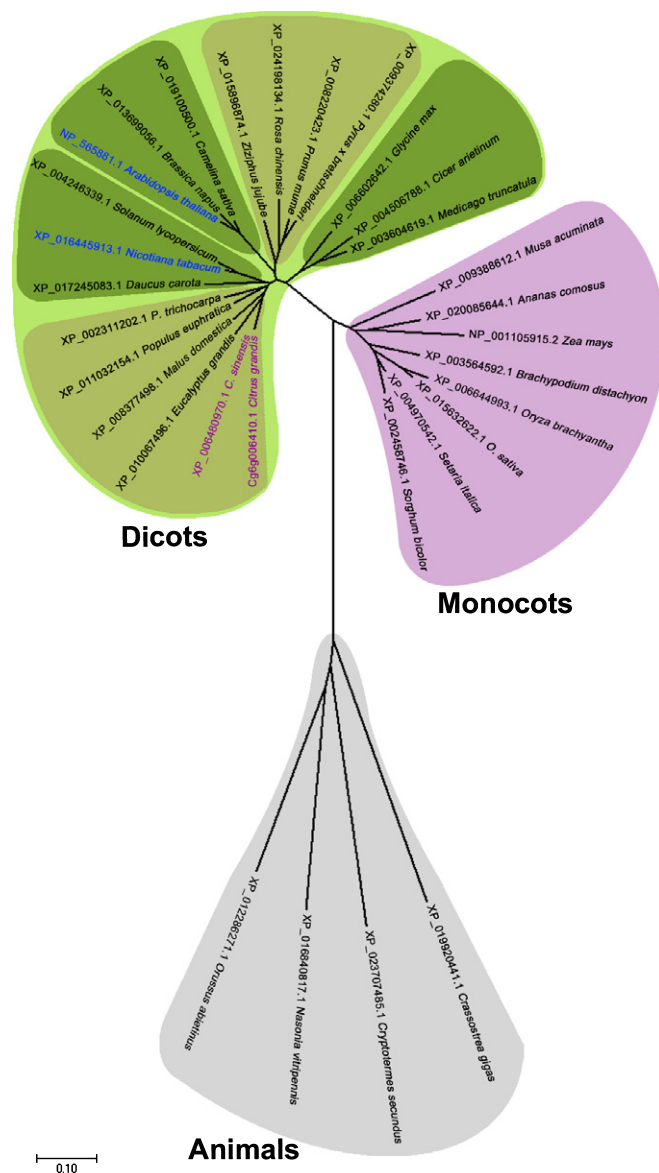


Fig. 2 Unrooted phylogenetic tree of *Citrus* LACCASE-4 (CsiLAC4) homologs by MEGA7 software (neighbor-joining method with 1000 bootstrap test). Subclustered herbaceous plant species are shown in deep green and woody plant species in brown. Bar, 0.10 substitution distance.

To further assess CsiLAC4 functions in B tolerance, we also treated mature plants of Col-0 and the *CsiLAC4^{OE}* lines with excessive boric acid. Surprisingly, boric acid excess stimulated early blooming and triggered precocious leaf senescence in the *CsiLAC4^{OE}* lines (Figs 3d, S8). At the end of boric acid treatment, the dry weight of aboveground plant parts was decreased in Col-0 treated with 5 mM boric acid. However, this phenomenon was not observed in the two *CsiLAC4^{OE}* lines (Fig. 3e).

CsiLAC4 but not CsiLAC17 contributes to cell wall lignification under boric acid excess

Boron excess had a profound phenotypic effect on hypocotyl elongation in the *CsiLAC4^{OE}* lines, leading us to slice and stain

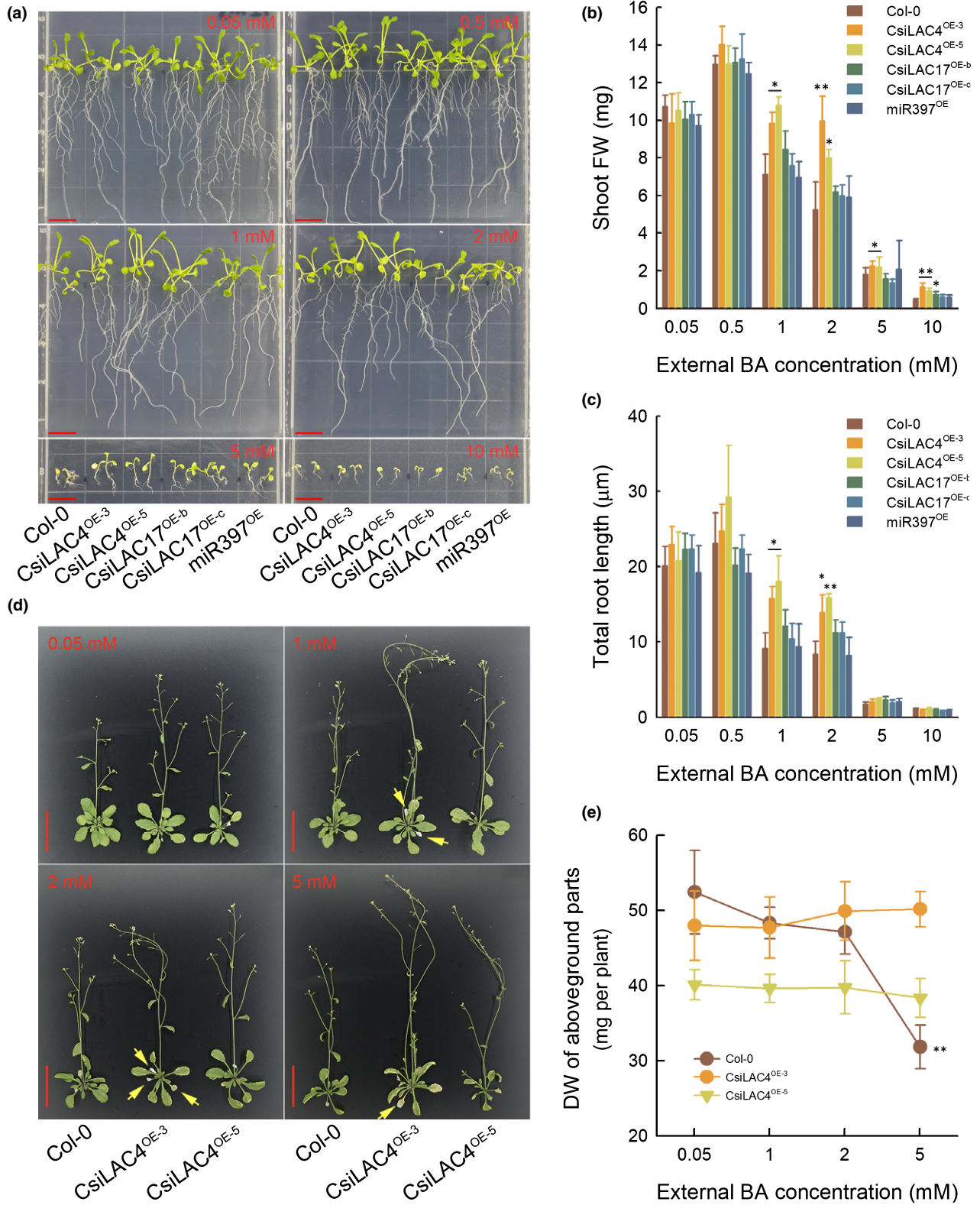


Fig. 3 Overexpression of *CsiLAC4* (*CsiLAC4*^{OE}) in *Arabidopsis* alleviates boric acid-toxic effects on plant growth and development at both young (a–c) and more mature (d, e) stages. (a) Sterilized seeds were sown on 1/2 Murashige & Skoog (1/2MS) solid medium containing different levels of boric acid and were vertically grown in a chamber under standard culture conditions (16 h photoperiod) for 14 d. Bar, 1 cm. (b) Shoot fresh weight (FW). (c) Total root length determined by the IMAGEJ software. (d) Three-week-old seedlings transplanted in 1 l plastic pots were irrigated with 100 ml of 1/2MS liquid medium supplemented with boric acid every other day for 14 d. Yellow arrowheads indicate early leaf senescence. Bar, 5 cm. (e) Dry weight (DW) of aboveground parts. Results are mean ± SD. Asterisks indicate significant differences at: *, *P* < 0.05; and **, *P* < 0.01 by one-way ANOVA (Student–Newman–Keuls method, *n* = 6).

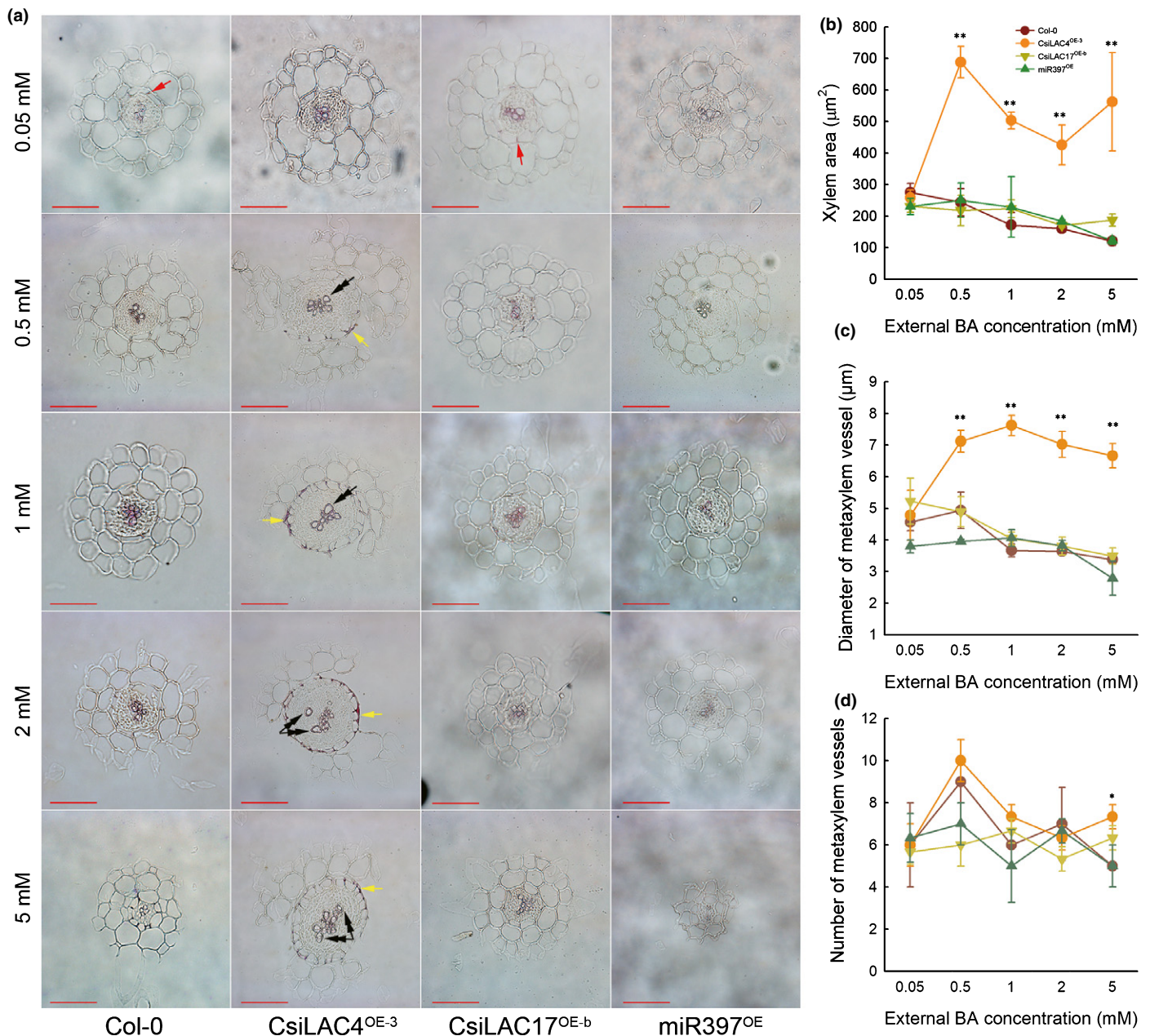


Fig. 4 Boric acid excess results in secondary xylem development and lignin deposition in the outer endodermal cell walls (yellow arrows) in the CsiLAC4^{OE} line, but not in the wild-type (Col-0), nor in CsiLAC17^{OE} and miR397^{OE} lines. (a) Primary roots from 14-d-old seedlings were transversely sectioned at the mature zone and stained with phloroglucinol-HCl. Red arrows indicate the Casparian strips. Double arrowheads indicate the metaxylem. Xylem area (b) and diameter of metaxylem vessels (c) were determined by IMAGEJ software, and the number of metaxylem vessels was hand-calculated. Results are mean \pm SD. Asterisks indicate significant differences at: *, $P < 0.05$; and **, $P < 0.01$ by one-way ANOVA (Student-Newman-Keuls method, $n = 4$). Bar, 50 μm .

the hypocotyl sections with phloroglucinol-HCl. We found that only lignified cell walls (including xylem cell walls and the Casparian strips in the endodermal cell walls) stained purple and that higher levels of external boric acid tended to decrease the size of xylem vessels in all the transgenic lines. Metaxylem vessels in the hypocotyls of CsiLAC4^{OE} plants were enlarged after exposure to excessive boric acid and were higher in number when external boric acid reached 5 mM (Fig. S9). Since anatomical structures of the roots and hypocotyls are highly similar in *Arabidopsis*, we also subjected the boric acid-treated primary root segments to paraffin

sections. Excessive boric acid treatments increased the stele diameter in CsiLAC4^{OE} primary roots (Fig. 4a), resulting in not only enlarged metaxylem vessels (Fig. 4b,c) but also B-dose-dependent lignification of the outer endodermal cell walls (Fig. 4a). By contrast, in Col-0 and miR397^{OE} lines, a 5 mM boric acid supplement in the growing medium suppressed stele development by decreasing the number and diameter of metaxylem vessels (Fig. 4a–d).

By monitoring their relative abundance, we found that mRNA levels of CsiLAC4 and CsiLAC17 did not correlate

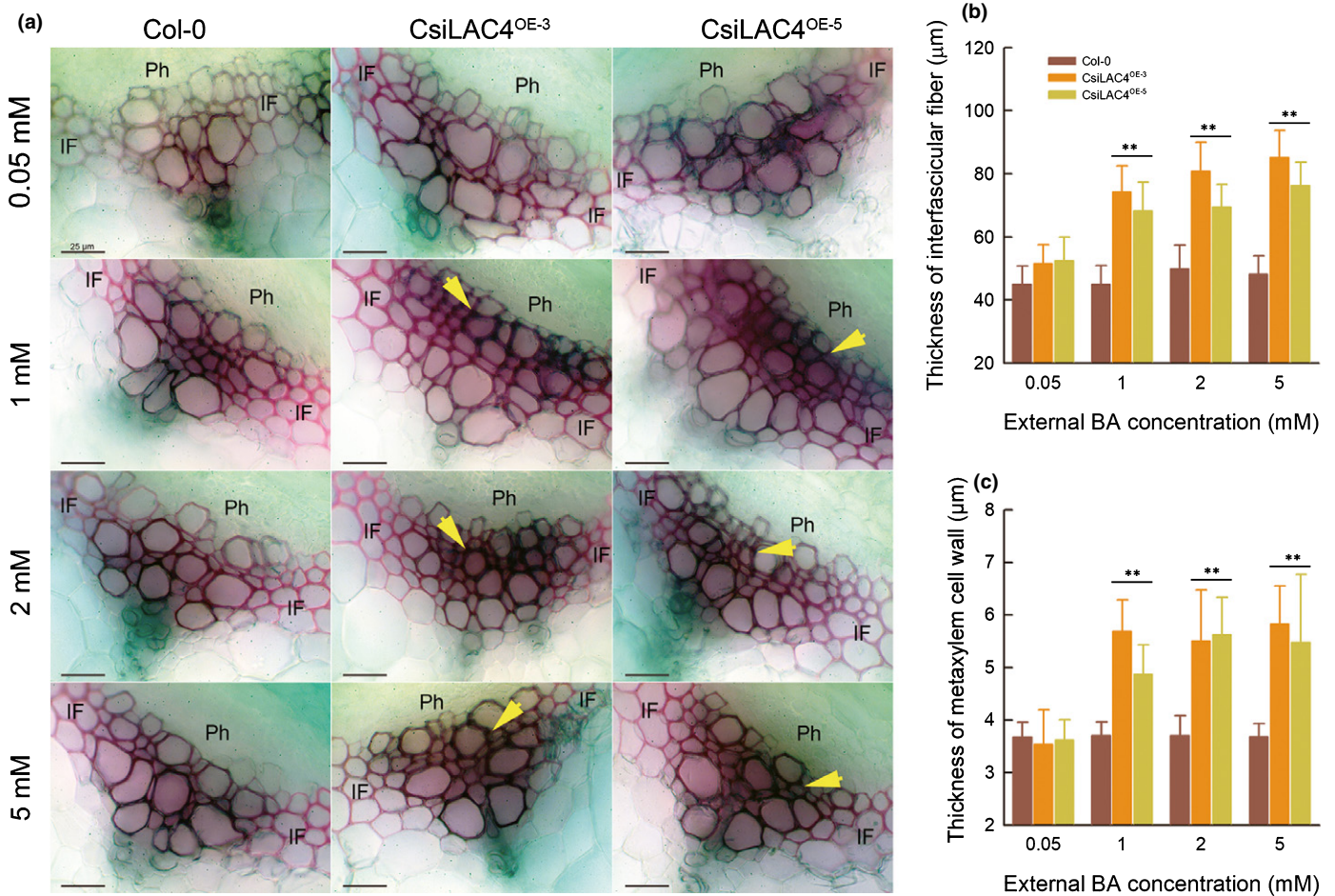


Fig. 5 Boric acid excess results in lignin deposition in metaxylem cell walls (yellow arrows) and increase in thickness of interfascicular fiber in inflorescence stems of CsiLAC4^{OE} lines. (a) Hand sections were cut from a mature inflorescence stem (5 cm above the rosette) 14 d after the boric acid treatment and were stained with phloroglucinol-HCl. (b, c) Thickness of interfascicular fiber (b) and xylem cell wall (c) were measured with the IMAGEJ software. Results are mean ± SD. Asterisks indicate significant differences at: **, P < 0.01 level by one-way ANOVA (Student-Newman-Keuls method, n = 4). Ph, phloem; IF, interfascicular fiber. Bar, 25 μm.

with external B levels in the roots or shoots of the corresponding transgenic lines (Figs S10a,b, S11). Given that Ath-miR397a shares 100% identity with Csi-miR397 (Fig. S10c), and that Ath-miR397a targets *AthLAC4* and *AthLAC17* in wild-type *Arabidopsis* (Wang *et al.*, 2014), we also monitored the expression of endogenous miR397a, *AthLAC4* and *AthLAC17* in the wild-type and transgenic *Arabidopsis* treated with excessive B. We found similar expression patterns of *AtLAC4* and *AtLAC17* for Col-0, CsiLAC4^{OE} and CsiLAC17^{OE} lines (Figs S10a,b, S11). In the roots, boric acid promoted expression of *AtLAC4* and *AtLAC17* for the plant lines, although both *AtLAC4* and *AtLAC17* were suppressed as boric acid increased. Nonetheless, lignification was only observed in the CsiLAC4^{OE} line, suggesting a minor contribution of *AthLAC4* and *AthLAC17* to the high-B-triggered lignification for the CsiLAC4^{OE} plants.

In mature inflorescent stems of CsiLAC4^{OE} lines, boric acid excess resulted in lignin deposition in the metaxylem, increasing the thickness of interfascicular fibers and the metaxylem cell walls (Figs 5, S12).

Cell wall lignification reduces water-soluble B in CsiLAC4^{OE} plants under boric acid excess

Previous reports showed that cell wall hydrophobicity correlates linearly with lignin content (Hyo & Tatsuko, 2010; Heiss-Blanquet *et al.*, 2011). Lignin deposition in the outer endodermal cell walls of boric acid-treated CsiLAC4^{OE} roots might set up an extracellular diffusion barrier for boric acid into the stele, thereby reducing B content in shoots. We determined the concentrations of water-soluble B, organic-bound B and cell wall-bound B in the boric acid-treated *Arabidopsis* samples (Martinez-Cuenca *et al.*, 2015). Our results indicated that the concentrations of all B fractions increased with the external boric acid concentrations in all tissue samples, except for cell wall-bound B in mature roots. Most B in the roots and shoots of young seedlings and rosette leaves and roots from mature plants appeared in the water-soluble fractions. Cell wall-bound B accounted for a relatively small proportion in the boric acid-treated samples. Organic-bound B increased in seedling roots, rosette leaves and roots from mature plants under boric acid excess. There was no

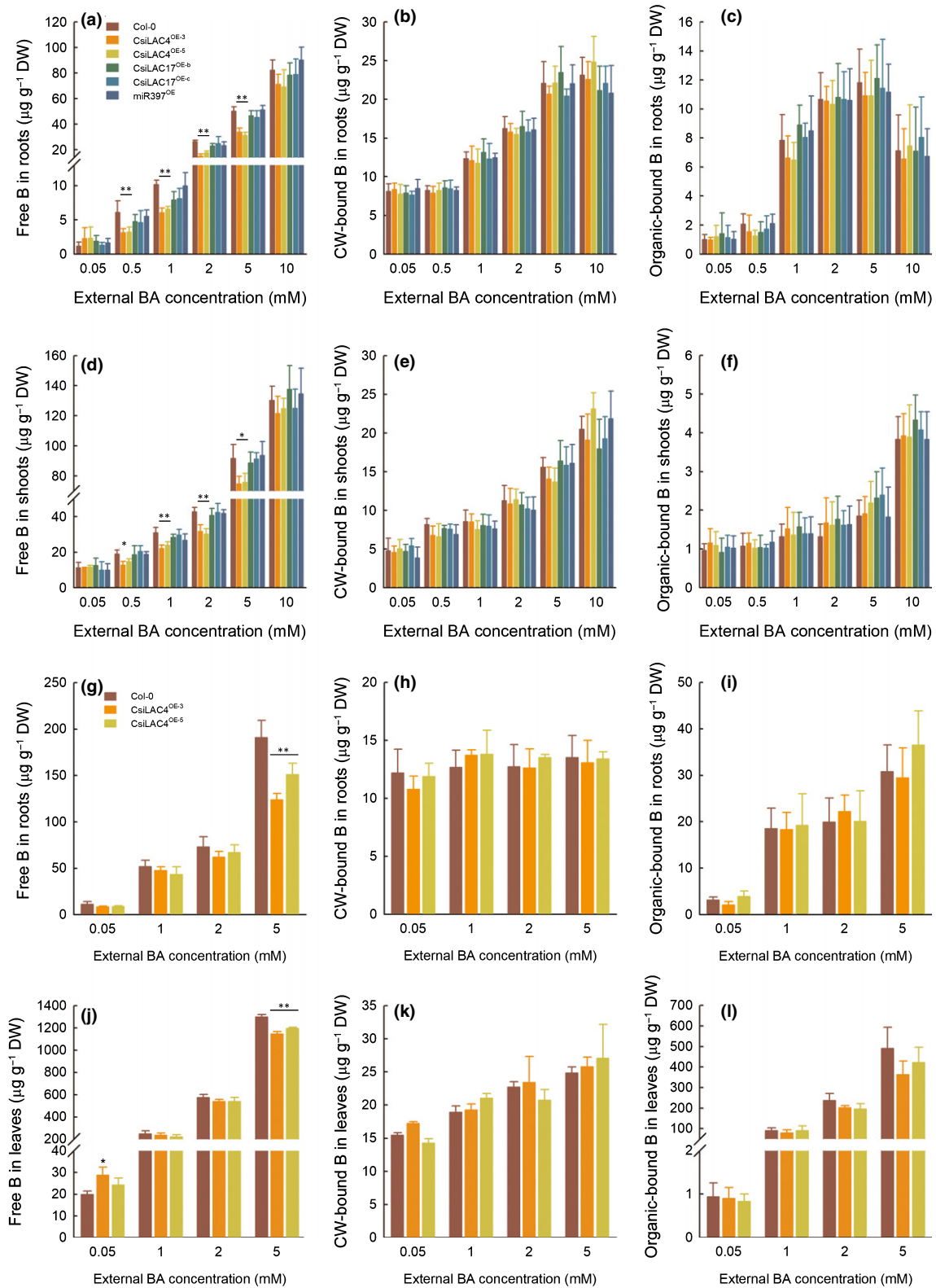


Fig. 6 Overexpression of *CsiLAC4* ($CsiLAC4^{OE}$), rather than of *CsiLAC17* ($CsiLAC17^{OE}$) and *pre-miR397* ($miR397^{OE}$) in *Arabidopsis*, decreases free boron (B) concentrations under excess boric acid treatments. B fractions in the root (a–c) and shoots (d–f) of 14-d-old seedlings, roots (g–i) and leaves (j–l) from mature plants were extracted as described by Martínez-Cuenca *et al.* (2015). All fractions were finally determined by inductively coupled plasma-MS. Free B in roots (a, d, g, j). Cell wall (CW)-bound B (b, e, h, k). Organic-bound B (c, f, i, l). Results are mean \pm SD. Asterisks indicate significant differences at: *, $P < 0.05$; and **, $P < 0.01$ by one-way ANOVA (Student-Newman-Keuls method, $n = 4$). FW, fresh weight; DW, dry weight.

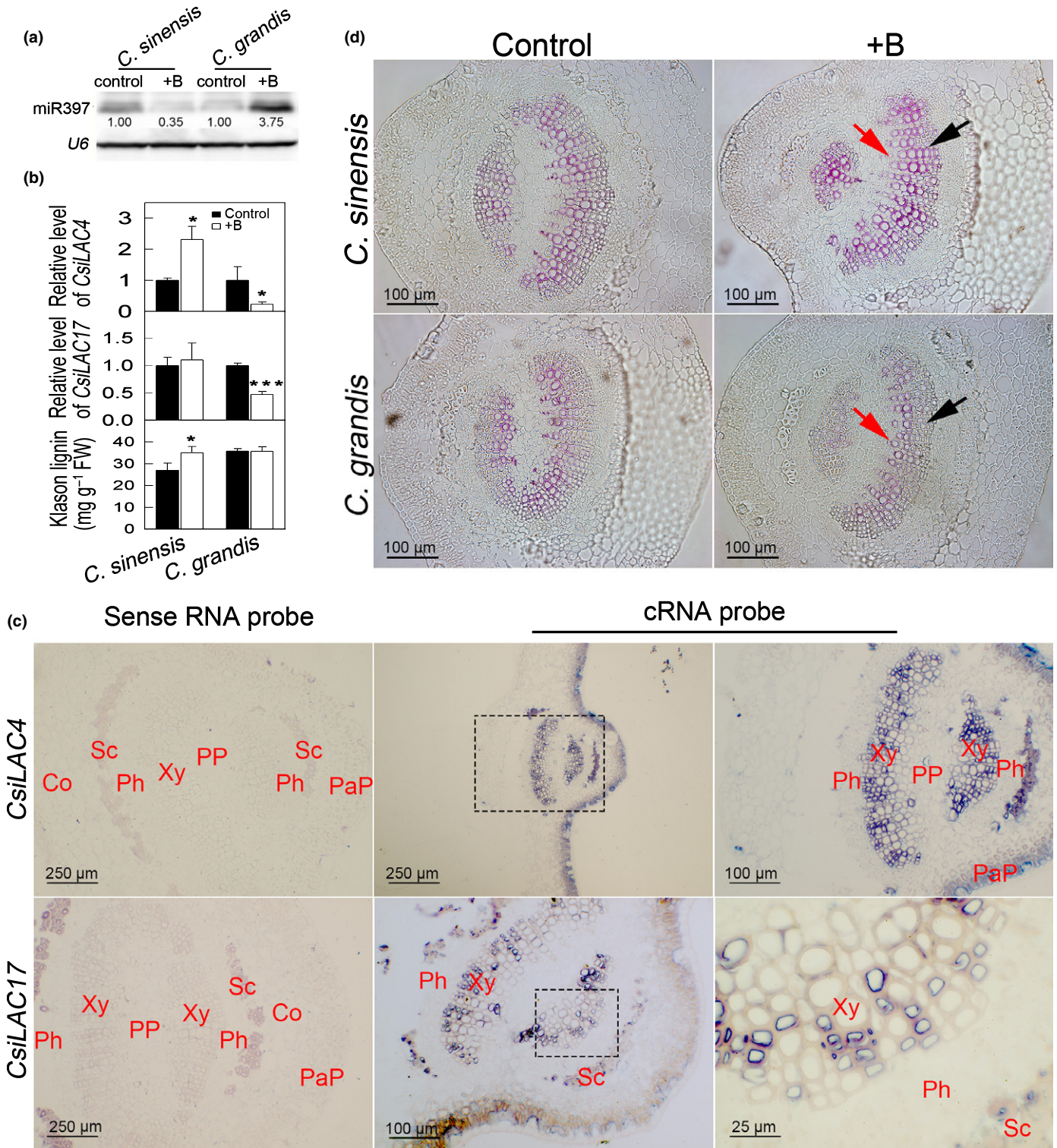


Fig. 7 Boric acid (BA)-responsive miR397 in *Citrus* leaves negatively modulates CsiLAC4, which contributes to lignification of the metaxylem parenchyma. (a) miRNA blotting. miR397 levels in BA-treated *Citrus sinensis* and *Citrus grandis* leaves. (b) Relative levels of CsiLAC4 and CsiLAC17 and Klason lignin content in responding to excessive BA treatments. (c) *In situ* mRNA hybridization showed that CsiLAC4 and CsiLAC17 are specifically expressed in the metaxylem. (d) BA treatment results in lignin deposition in the metaxylem according to phloroglucinol-HCl staining. Co, cortex; PaP, palisade parenchyma; Ph, phloem; PP, pith parenchyma; Sc, sclerenchyma; Xy, xylem. Black arrows indicate the metaxylem, while red arrows indicate the protoxylem. Results are mean \pm SD. Asterisks indicate significant differences at: *, $P < 0.05$; and ***, $P < 0.001$ by independent sample *t*-tests ($n = 3$).

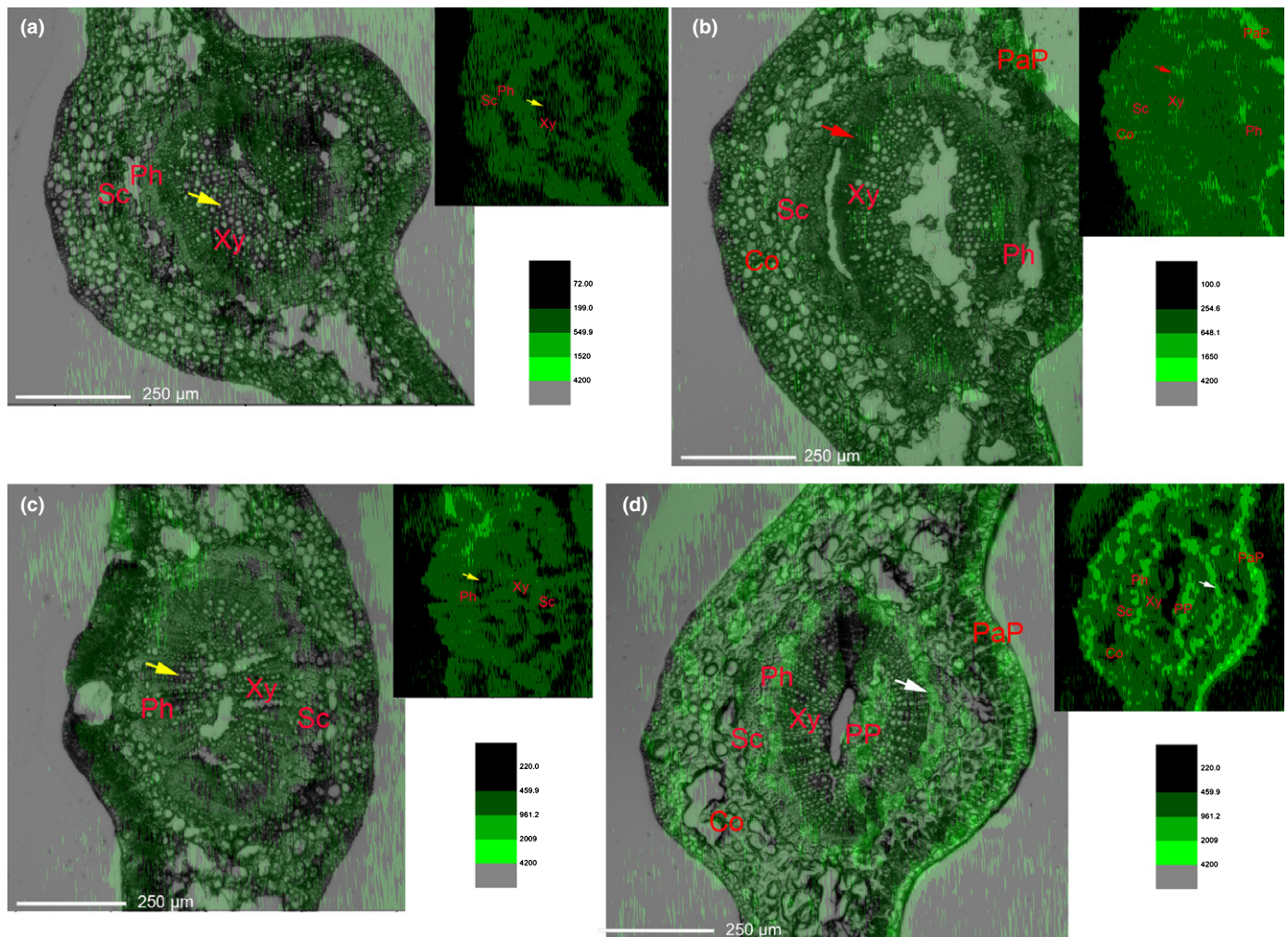


Fig. 8 *In situ* boron (B) distribution in transverse *Citrus* leaf sections. Bright-field micrographs of leaf sections were overlaid with corresponding B distribution contours (top right), generated from laser ablation-inductively coupled plasma-MS data by ORIGINPRO software (v.9.0.0). Relatively weak B signals (yellow arrows) were detected in the control xylem of both *Citrus sinensis* (a) and *Citrus grandis* (c). Excessive boric acid treatment results in stronger B signals in the metaxylem of *C. sinensis* (red arrows) (b), and much stronger B signals in the phloem of *C. grandis* (white arrows) (d). PaP, palisade parenchyma; Ph, phloem; PP, pith parenchyma; Sc, sclerenchyma; Xy, xylem. Similar results were obtained from three biological repeats.

significant difference for organic-bound B and cell wall-bound B between Col-0 and the transgenic plants under the same external boric acid levels; however, water-soluble B was significantly lower in the *CsiLAC4*^{OE} lines under the same conditions (Fig. 6).

CsiLAC4 triggers xylem cell wall lignification in *Citrus* under boric acid excess

We used miRNA blotting to show that excessive boric acid downregulated miR397 in *C. sinensis* but upregulated it in *C. grandis* (Fig. 7a), which negatively regulated expression of *CsiLAC4* and *CsiLAC17* (Fig. 7b). To examine the tissue specificity of *CsiLAC4* and *CsiLAC17* expressions, we conducted mRNA *in situ* hybridization on transverse leaf sections. The results showed that *CsiLAC4* and *CsiLAC17* were specifically expressed in the xylem parenchyma cells (Fig. 7c). Boric acid excess resulted in a significant increase of lignin content in *C. sinensis* (Fig. 7b). To verify that such

lignification was caused by differential expression of *CsiLAC4*, we profiled expressions of laccase-like family genes in the boric acid-treated *Citrus* leaves. We obtained 34 laccase-like family members from the *Citrus* genomic database and clustered them into six groups by bioinformatics analysis (Fig. S13a). *CsiLAC4* was the only gene upregulated in boric acid-treated *C. sinensis* leaves, accompanied by downregulation of *Cs1g01800* and *Cs2g29090*, which are predicted to be involved in the oxidation–reduction process. Although most of the laccase-like members in group 6 were upregulated in *C. grandis* leaves in response to the boric acid treatment, they did not affect lignin content in the leaves (Figs 7b, S11, S13b,c). These results suggested a contribution of *CsiLAC4* to lignification in *C. sinensis* leaves. The effects of *CsiLAC4* on lignification were evaluated by the histochemical method. Wiesner's staining revealed a substantial lignin deposition in the metaxylem of boric acid-treated *C. sinensis* leaves but not in *C. grandis* (Fig. 7d).

Secondary lignification of xylem changes B distribution in *Citrus* leaves

To test our hypothesis that cell wall lignification modulates B flow, we monitored the *in situ* B distribution in *Citrus* leaves by LA-ICP-MS. Rebuilt images from mass spectra data showed a similar B distribution pattern in control leaf veins in *C. grandis* and *C. sinensis*. The lignified tissues (xylem and sclerenchyma) maintained relatively lower levels of B when compared to thin-walled tissue (such as phloem and storage parenchyma) (Fig. 8a, c). Unlike this pattern, lignification in boric acid-treated *C. sinensis* leaves resulted in relatively higher B levels in the xylem (particularly the metaxylem) compared to the surrounding tissues. The highest B levels in treated *C. sinensis* leaves were detected in the palisade parenchyma tissue (Fig. 8b). However, in boric acid-treated *C. grandis* leaves, the discrepancy in B distribution was clear – most B was detected in palisade parenchyma, phloem and pith (Fig. 8d).

Discussion

Plants have two essential strategies to deal with B excess: decrease B content *in vivo* by efflux transporters and chelate the excessive free B by organic compounds (Hayes & Reid, 2004; Papadakis *et al.*, 2018). Speculations regarding B compartmentalization in the extracellular regions or the vacuoles are ultimately efflux-based (Reid & Fitzpatrick, 2009; Martinez-Cuenca *et al.*, 2015). Here we provided strong evidence supporting a novel strategy for plants to cope with B excess, in which *CsiLAC4* modulates free B flow via lignifying cell walls.

Lignins are cell wall phenolic heteropolymers resulting from the oxidative coupling of three monolignols (Barceló *et al.*, 2004). These phenolic heteropolymers contain various oxygen groups such as hydroxyl, carboxyl, methoxyl and aldehyde that can couple to heavy metal ions to form stable chemical bonds (Sarkanen & Ludwig, 1971; Memon & Schroder, 2009). Lignin biosynthesis in plants plays an important role in detoxifying excess heavy metal ions (e.g. copper, zinc and manganese) through binding the ions in the extracellular regions (van de Mortel *et al.*, 2006; Gao *et al.*, 2012; Liu *et al.*, 2014). Notably, lignin's affinity with heavy metal ions is strongly dependent on pH and ionic strength (Guo *et al.*, 2008). In dicots, boric acid forms stable borates with important lignin precursors such as caffeic and hydroxiferulic acids (Bolaños *et al.*, 2004). Consequently, boric acid in plants might be bound to lignin in the extracellular regions. However, a similar detoxifying mechanism of lignin for excessive boric acid is still unknown due to the absence of evidence for binding of B to lignin (Ghanati *et al.*, 2005; Cervilla *et al.*, 2009).

We confirmed that *CsiLAC4* and *CsiLAC17* are two sterling targets of miR397 (Fig. 1). Although these two genes belong to the laccase-like family, their coding proteins are different from their homologs in *Arabidopsis* (Fig. S2). Similar to the overexpressions of *AtLAC4* and *AtLAC17* in Col-0 background *Arabidopsis*, overexpressing either *CsiLAC4* or *CsiLAC17* in *Arabidopsis* did not produce an observable phenotype (Benske, 2014).

Nonetheless, overexpression of *CsiLAC4* (rather than *CsiLAC17*) in *Arabidopsis* contributed to the tolerance of the transgenic plants to B excess (Fig. 3). This could be attributed to their low similarity in protein sequence (*CsiLAC4* shares 58.7% identity with *CsiLAC17*; Figs S2, S13a). *CsiLAC4* in *Arabidopsis* lignified the outer endodermal cell walls, metaxylem and interfascicular fibers (Figs 4, 5, S9, S10), possibly by binding itself to the lignifying cell wall and polymerizing lignin precursors (O'Malley *et al.*, 1993). This process, however, seemed not to be able to bind B to the extracellular regions because cell wall-bound B concentrations in the roots and shoots of *CsiLAC4*^{OE} did not differ from other lines. Nevertheless, a significant decrease of water-soluble B in the roots and shoots of *CsiLAC4*^{OE} seedlings suggests that high B-triggered lignification in the outer endodermal cell walls efficiently suppressed boric acid penetration across the endodermis into stele as well as upward transport of boric acid into shoots (Fig. 6).

Our results support the detoxifying mechanism exerted by B-chelating compounds in *Arabidopsis*. As shown in Fig. 6(i,l), organically bound B in the roots and rosette leaves was dramatically increased after the boric acid treatments. In young seedlings, organically bound B in the shoots increased when the external boric acid level reached 10 mM (Fig. 6f), possibly due to its relatively small participation in secondary metabolism and the fact that metabolites might be transported into roots to chelate B (Fig. 6c). The lower water-soluble and organically bound B in rosette leaves of the *CsiLAC4*^{OE} lines suggested that lignification in roots might function as an increased 'physical barrier' preventing B from flowing into the plant by upward transport. By measuring concentrations of other mineral nutrients, we found that total B, Mg, Mn and Zn in rosette leaves decreased in response to the boric acid treatment (Fig. S14a,c,e,p). In the roots, boric acid reduces only total B and Mg content, although it binds more Ca, Mn, Cu and Zn into the cell walls for the *CsiLAC4*^{OE} lines (Fig. S14f,l-o,q). The results suggest that lignification in the roots modulates upward transport of mineral nutrients by binding metal ions and absorbing nutrients by setting up physical barriers to ionic (Mg²⁺) and nonionic (B) flow.

It was found that boric acid toxicity induces ethylene-related gene expression in plants and might trigger oxidative stress-adaptive responses in *Arabidopsis* by miRNA-based modulation of ethylene biosynthesis (Öz *et al.*, 2009; Kayihan *et al.*, 2017; Kayihan *et al.*, 2019). In *CsiLAC4*^{OE} lines, we noted that boric acid excess resulted in hypocotyl and root elongation of the young seedlings, early flowering, and precocious leaf senescence of mature plants (Fig. 3). Such developmental phenomena are related to the stress hormone ethylene (Ogawara *et al.*, 2003; Vandebussche *et al.*, 2012; Koyama, 2014). The salt stress treatment, which could induce ethylene biosynthesis, showed that the elongation of hypocotyls in the *CsiLAC4*^{OE} lines was much more prominent, implying that *CsiLAC4* might be involved in the responses of *CsiLAC4*^{OE} plants to ethylene (Fig. S7) (Tao *et al.*, 2015). Recently, Pandey *et al.* (2021) reported that the redistribution of volatile ethylene in compacted soil can influence plant growth and development. Similarly, cell wall lignification might alter ethylene diffusion within the boric acid-treated *CsiLAC4*^{OE}

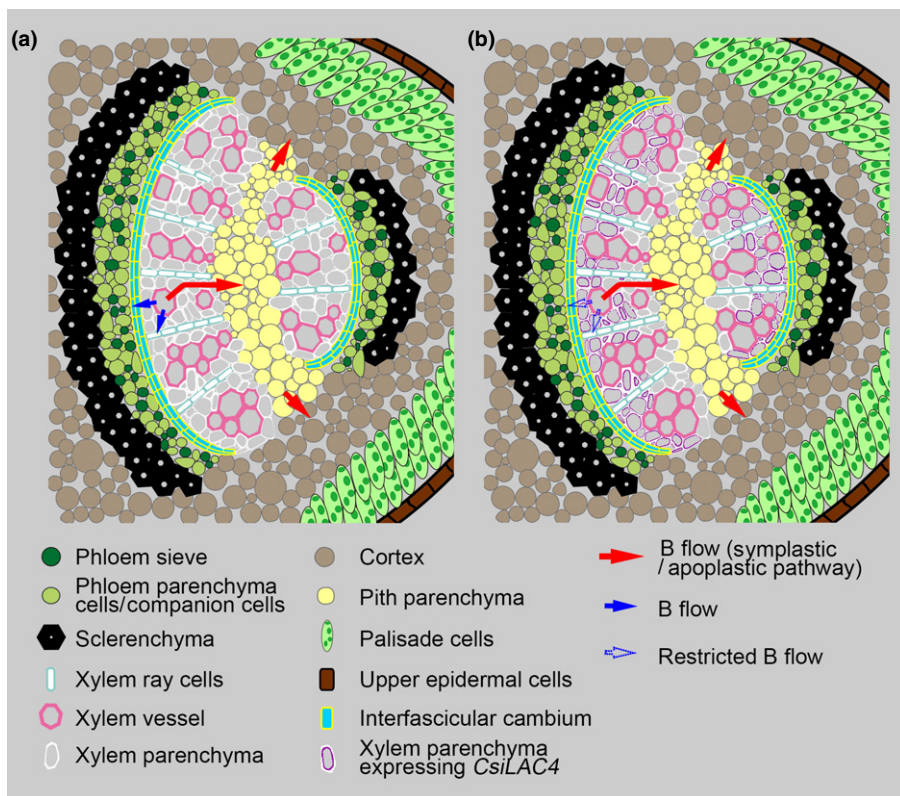


Fig. 9 Suggested model for the role of *CsiLAC4* in the preferential distribution of boron (B) in *Citrus* leaves. (a) Schematic diagram of B distribution in B-intolerant *Citrus grandis* main veins. B in the xylem vessel is first unloaded into the xylem parenchyma by either equilibration or active transport, followed by further transfer to the phloem and pith parenchyma within the symplast. (b) Schematic diagram of B distribution in B-tolerant *Citrus sinensis* main veins. Boric acid treatment triggers cell wall lignification of metaxylem parenchyma expressing *CsiLAC4*, which restricts B flow between the xylem/apoplast interface and further transfer to the phloem.

plants, thereby triggering hormone responses. Given that ethylene is involved in modulating the onset of leaf senescence and may play antagonistic roles in regulating plant tolerance to stresses, the altered ethylene distribution may further explain why, under excessive boric acid concentrations, *CsiLAC4*^{OE} plants still showed severe leaf chlorosis and senescence, even though they maintained lowered water-soluble and organic-bound B concentrations (Fig. 3d,e,g) (Koyama, 2014; Tao *et al.*, 2015).

Given that the majority of B in xylem existed in a water-soluble form, our findings in *Citrus* provided evidence that lignification of the xylem might restrict outward transport of B (Figs 7d, 8b), which seemed to be independent from B fixation by the lignin in cell walls, since the cell wall-bound B content in boric acid-treated *C. sinensis* leaves was similar to that in the control (Table S6).

For B distribution within *Citrus*, our findings have several implications summarized in the model shown in Fig. 9. Given that boric acid-induced secondary lignin in *C. sinensis* leaves was deposited specifically in the xylem parenchyma cell wall toward the vessel pits (the xylem/symplast interface) (Huang *et al.*, 2016), lignification would alter the B flow between the apoplast (xylem vessel) and symplast (xylem parenchyma cells) by changing the permeability, thereby restricting further transfer of B from the symplast of xylem parenchyma into the phloem by either the symplastic or apoplastic pathway (Figs 7d, 8b,d). For radial B transport, the phloem, palisade tissue and pith might act as buffering pools under excessive boric acid conditions (Fig. 8d). In B-phloem-mobile species, the phloem can reallocate B from

matured organs to developing young ones (Brown & Shelp, 1997). However, the phloem of *Citrus* seemed incapable of delivering B to other organs under boric acid excess, possibly due to its inability to chelate B to organic compounds (Table S6).

In conclusion, our results showed that *CsiLAC4* contributes to plant tolerance to B excess by lignifying cell walls, which might set up a 'physical barrier' preventing the free B flow out of the xylem.

Acknowledgements


We thank Dr Chong Zhang for providing the pBI121-DsRed/GFP vectors; Dr Wei Wang for help with miRNA blotting; Bi-Fei Huang for technical assistance with LA-ICP-MS analysis; and Dr Yuan Li and the anonymous reviewers for critical comments and suggestions on the manuscript. This work was supported by the National Natural Science Foundation of China (31701901), Collaborative Innovation Project from PGFP & CAAS (XTCXGC2021006), the Science and Technology Innovation Team of FAAS (CXTD2021003-3), and the State Scholarship Fund by the China Scholarship Council (201909350003).

Author contributions


J-HH, G-CF and L-SC designed the research; J-HH and L-YZ conducted the experiments; X-JL, YG and DZ participated in the phenotypic analysis, anatomical studies and RT-PCR; JZ participated in lignin determination; W-LH performed B determination; J-HH wrote the manuscript; L-SC and RSF revised and


edited the manuscript. All authors reviewed and accepted the final version of the manuscript.

ORCID

Li-Song Chen  <https://orcid.org/0000-0001-8425-1306>

Rhuanito Soranz Ferrarezi  <https://orcid.org/0000-0002-6873-7995>

Jing-Hao Huang  <https://orcid.org/0000-0001-6983-612X>

Xiong-Jie Lin  <https://orcid.org/0000-0002-2060-1087>

Data availability

Data are available in the article's Supporting Information.

References

- Barceló AR, Ros LVG, Gabaldón C, López-Serrano M, Pomar F, Carrión JS, Pedreño MA. 2004. Basic peroxidases: the gateway for lignin evolution? *Phytochemistry Reviews* 3: 61–78.
- Benske A. 2014. *Laccase-dependent lignification of secondary cell walls of protoxylem tracheary elements in Arabidopsis thaliana*. MSc thesis, University of British Columbia, Vancouver, BC, Canada.
- Berthet S, Demont-Caulet N, Pollet B, Bidzinski P, Cezard L, Le Bris P, Borrega N, Herve J, Blondet E, Balzergue S *et al.* 2011. Disruption of LACCASE4 and 17 results in tissue-specific alterations to lignification of *Arabidopsis thaliana* stems. *Plant Cell* 23: 1124–1137.
- Bingham FT, Strong JE, Rhoades JD, Keren R. 1987. Effects of salinity and varying boron concentrations on boron uptake and growth of wheat. *Plant and Soil* 97: 345–351.
- Bolaños L, Lukaszewski K, Bonilla I, Blevins D. 2004. Why boron? *Plant Physiology and Biochemistry* 42: 907–912.
- Braissant O, Wahli W. 1998. A simplified *in situ* hybridization protocol using non-radioactively labelled probes to detect abundant and rare mRNAs on tissue sections. *Biochemica* 1: 10–16.
- Brdar-Jokanovic M. 2020. Boron toxicity and deficiency in agricultural plants. *International Journal of Molecular Sciences* 21: 1424.
- Brown PH, Shelp BJ. 1997. Boron mobility in plants. *Plant and Soil* 193: 85–101.
- Cervilla LM, Rosales MA, Rubio-Wilhelmi MM, Sanchez-Rodriguez E, Blasco B, Rios JJ, Romero L, Ruiz JM. 2009. Involvement of lignification and membrane permeability in the tomato root response to boron toxicity. *Plant Science* 176: 545–552.
- Chatterjee M, Tabi Z, Galli M, Malcomber S, Buck A, Muszynski M, Gallavotti A. 2014. The boron efflux transporter ROTTEN EAR is required for maize inflorescence development and fertility. *Plant Cell* 26: 2962–2977.
- Chen L-S, Han S, Qi Y-P, Yang L-T. 2012. Boron stresses and tolerance in citrus. *African Journal of Biotechnology* 11: 5961–5969.
- Durbak AR, Phillips KA, Pike S, O'Neill MA, Mares J, Gallavotti A, Malcomber ST, Gassmann W, McSteen P. 2014. Transport of boron by the *tassel-less1* aquaporin is critical for vegetative and reproductive development in maize. *Plant Cell* 26: 2978–2995.
- Eamens AL, Smith NA, Dennis ES, Wassenegeger M, Wang MB. 2014. In *Nicotiana* species, an artificial microRNA corresponding to the virulence modulating region of *Potato spindle tuber viroid* directs RNA silencing of a soluble inorganic pyrophosphatase gene and the development of abnormal phenotypes. *Virology* 450–451: 266–277.
- Fei Q, Yu Y, Liu L, Zhang Y, Baldrich P, Dai Q, Chen X, Meyers BC. 2018. Biogenesis of a 22-nt microRNA in *Phaseoleae* species by precursor-programmed uridylation. *Proceedings of the National Academy of Sciences, USA* 115: 8037–8042.
- Gao L, Peng K, Chen YQ, Wang G, Shen Z. 2012. Roles of apoplastic peroxidases, laccases, and lignification in the manganese tolerance of hyperaccumulator *Phytolacca americana*. *Acta Physiologiae Plantarum* 34: 151–159.
- Ghanati F, Morita A, Yokota H. 2005. Deposition of suberin in roots of soybean induced by excess boron. *Plant Science* 168: 397–405.
- Guo P, Qi YP, Yang LT, Ye X, Jiang HX, Huang JH, Chen LS. 2014. cDNA-AFLP analysis reveals the adaptive responses of citrus to long-term boron-toxicity. *BMC Plant Biology* 14: 284.
- Guo X, Zhang S, Shan XQ. 2008. Adsorption of metal ions on lignin. *Journal of Hazardous Materials* 151: 134–142.
- Han S, Tang N, Jiang H-X, Yang L-T, Li Y, Chen L-S. 2009. CO₂ assimilation, photosystem II photochemistry, carbohydrate metabolism and antioxidant system of citrus leaves in response to boron stress. *Plant Science* 176: 143–153.
- Hatfield RD, Jung HG, Ralph J, Buxton DR, Weimer PJ. 1994. A comparison of the insoluble residues produced by the Klason lignin and acid detergent lignin procedures. *Journal of the Science of Food and Agriculture* 65: 51–58.
- Hayes JE, Reid RJ. 2004. Boron tolerance in barley is mediated by efflux of boron from the roots. *Plant Physiology* 136: 3376–3382.
- Heiss-Blanquet S, Zheng D, Lopes Ferreira N, Lapierre C, Baumberger S. 2011. Effect of pretreatment and enzymatic hydrolysis of wheat straw on cell wall composition, hydrophobicity and cellulase adsorption. *Bioresource Technology* 102: 5938–5946.
- Huang J-H, Cai ZJ, Wen SX, Guo P, Ye X, Lin GZ, Chen LS. 2014. Effects of boron toxicity on root and leaf anatomy in two *Citrus* species differing in boron tolerance. *Trees-Structure and Function* 28: 1653–1666.
- Huang J-H, Lin X-J, Zhang L-Y, Wang X-D, Fan G-C, Chen L-S. 2019a. MicroRNA sequencing revealed *Citrus* adaptation to long-term boron toxicity through modulation of root development by miR319 and miR171. *International Journal of Molecular Sciences* 20: 1422.
- Huang J-H, Qi YP, Wen SX, Guo P, Chen XM, Chen LS. 2016. Illumina microRNA profiles reveal the involvement of miR397a in *Citrus* adaptation to long-term boron toxicity via modulating secondary cell-wall biosynthesis. *Scientific Reports* 6: 22900.
- Huang J-H, Xu J, Ye X, Luo TY, Ren LH, Fan GC, Qi YP, Li Q, Ferrarezi RS, Chen L-S. 2019b. Magnesium deficiency affects secondary lignification of the vascular system in *Citrus sinensis* seedlings. *Trees – Structure and Function* 33: 171–182.
- Hyo H, Tatsuko H. 2010. Lignin structure, properties, and applications. In: Abe A, Dusek K, Kobayashi S, eds. *Biopolymers: lignin, proteins, bioactive nanocomposites*. Berlin/Heidelberg, Germany: Springer, 1–63.
- Joseph JT, Poolakkalady NJ, Shah JM. 2018. Plant reference genes for development and stress response studies. *Journal of Biosciences* 43: 173–187.
- Kato Y, Miwa K, Takano J, Wada M, Fujiwara T. 2009. Highly boron deficiency-tolerant plants generated by enhanced expression of NIP5;1, a boric acid channel. *Plant and Cell Physiology* 50: 58–66.
- Kayihan C, Öz MT, Eyidoğan F, Yücel M, Öktem HA. 2017. Physiological, biochemical, and transcriptomic responses to boron toxicity in leaf and root tissues of contrasting wheat cultivars. *Plant Molecular Biology Reporter* 35: 97–109.
- Kayihan DS, Kayihan C, Özden Çiftçi Y. 2019. Moderate level of toxic boron causes differential regulation of microRNAs related to jasmonate and ethylene metabolisms in *Arabidopsis thaliana*. *Turkish Journal of Botany* 43: 167–172.
- Koyama T. 2014. The roles of ethylene and transcription factors in the regulation of onset of leaf senescence. *Frontiers in Plant Science* 5: 650.
- Kumar S, Stecher G, Tamura K. 2016. MEGA7: molecular evolutionary genetics analysis v.7.0 for bigger datasets. *Molecular Biology and Evolution* 33: 1870–1874.
- Landi M, Margaritopoulou T, Papadakis IE, Araniti F. 2019. Boron toxicity in higher plants: an update. *Planta* 250: 1011–1032.
- Li Y, Han M-Q, Lin F, Ten Y, Lin J, Zhu D-H, Guo P, Weng YB, Chen L-S. 2015. Soil chemical properties, 'Guanximiyou' pummelo leaf mineral nutrient status and fruit quality in the southern region of Fujian province, China. *Journal of Soil Science and Plant Nutrition* 15: 615–628.
- Liu Q, Zheng L, He F, Zhao F, Shen Z, Zheng L. 2014. Transcriptional and physiological analyses identify a regulatory role for hydrogen peroxide in the lignin biosynthesis of copper-stressed rice roots. *Plant and Soil* 387: 323–336.

- Llave C, Xie Z, Kasschau KD, Carrington JC. 2002. Cleavage of *Scarecrow-like* mRNA targets directed by a class of *Arabidopsis* miRNA. *Science* 297: 2053–2056.
- Loomis WD, Durst RW. 1992. Chemistry and biology of boron. *BioFactors* 3: 229–239.
- Martinez-Cuenca MR, Martinez-Alcantara B, Quinones A, Ruiz M, Iglesias DJ, Primo-Millo E, Forner-Giner MA. 2015. Physiological and molecular responses to excess boron in *Citrus macrophylla* W. *PLoS ONE* 10: e0134372.
- Mayer AM, Staples RC. 2002. Laccase: new functions for an old enzyme. *Phytochemistry* 60: 551–565.
- Memon AR, Schroder P. 2009. Implications of metal accumulation mechanisms to phytoremediation. *Environmental Science and Pollution Research International* 16: 162–175.
- Miwa K, Aibara I, Fujiwara T. 2014. *Arabidopsis thaliana* BOR4 is upregulated under high boron conditions and confers tolerance to high boron. *Soil Science and Plant Nutrition* 60: 349–355.
- Miwa K, Takano J, Omori H, Seki M, Shinozaki K, Fujiwara T. 2007. Plants tolerant of high boron levels. *Science* 318: 1417.
- van de Mortel JE, Almar Villanueva L, Schat H, Kwekkeboom J, Coughlan S, Moerland PD, Loren V, van Themaat E, Koornneef M, Aarts MG. 2006. Large expression differences in genes for iron and zinc homeostasis, stress response, and lignin biosynthesis distinguish roots of *Arabidopsis thaliana* and the related metal hyperaccumulator *Thlaspi caerulescens*. *Plant Physiology* 142: 1127–1147.
- Nable RO, Bañuelos GS, Paull JG. 1997. Boron toxicity. *Plant and Soil* 193: 181–198.
- Nable RO, Paull JG, Cartwright B. 1990. Problems associated with the use of foliar analysis for diagnosing boron toxicity in barley. *Plant and Soil* 128: 225–232.
- Ochiai K, Shimizu A, Okumoto Y, Fujiwara T, Matoh T. 2011. Suppression of a NAC-like transcription factor gene improves boron-toxicity tolerance in rice. *Plant Physiology* 156: 1457–1463.
- Ogawara T, Higashi K, Kamada H, Ezura H. 2003. Ethylene advances the transition from vegetative growth to flowering in *Arabidopsis thaliana*. *Journal of Plant Physiology* 160: 1335–1340.
- O'Malley DM, Whetten R, Bao W, Chen CL, Sederoff RR. 1993. The role of laccase in lignification. *The Plant Journal* 4: 751–757.
- Öz MT, Yilmaz R, Eyidoğan F, De Graaff L, Yücel M, Öktem HA. 2009. Microarray analysis of late response to boron toxicity in barley (*Hordeum vulgare* L.) leaves. *Turkish Journal of Agriculture and Forestry* 33: 191–202.
- Pandey BK, Huang G, Bhosale R, Hartman S, Sturrock CJ, Jose L, Martin OC, Karady M, Voesenek LACJ, Ljung K *et al.* 2021. Plant roots sense soil compaction through restricted ethylene diffusion. *Science* 371: 276–280.
- Papadakis IE, Dimassi KN, Bosabalidis AM, Therios IN, Patakas A, Giannakoula A. 2004. Boron toxicity in 'Clementine' mandarin plants grafted on two rootstocks. *Plant Science* 166: 539–547.
- Papadakis IE, Tsiantas PI, Tsaniklidis G, Landi M, Psychoyou M, Fasseas C. 2018. Changes in sugar metabolism associated to stem bark thickening partially assist young tissues of *Eriobotrya japonica* seedlings under boron stress. *Journal of Plant Physiology* 231: 337–345.
- Princi MP, Lupini A, Araniti F, Longo C, Mauceri A, Sunseri F, Abenavoli MR. 2016. Boron toxicity and tolerance in plants: recent advances and future perspectives. In: Ahmad P, ed. *Plant metal interaction*. Amsterdam, the Netherlands: Elsevier, 115–147.
- Raven JA. 1980. Short- and long-distance transport of boric acid in plants. *New Phytologist* 84: 231–249.
- Reid R. 2014. Understanding the boron transport network in plants. *Plant and Soil* 385: 1–13.
- Reid RJ, Fitzpatrick KL. 2009. Redistribution of boron in leaves reduces boron toxicity. *Plant Signaling & Behavior* 4: 1091–1093.
- Saleem M, Khanif YM, Fauziah I, Samsuri AW, Hafeez B. 2011. Importance of boron for agriculture productivity: a review. *International Research Journal of Agricultural Science and Soil Science* 1: 293–300.
- Sarkanen KV, Ludwig CH. 1971. *Lignins. Occurrence, formation, structure, and reactions*. New York, NY, USA: Wiley-Interscience.
- Schuetz M, Benske A, Smith RA, Watanabe Y, Tobimatsu Y, Ralph J, Demura T, Ellis B, Samuels AL. 2014. Laccases direct lignification in the discrete secondary cell wall domains of protoxylem. *Plant Physiology* 166: 798–807.
- Sheng O, Zhou G, Wei Q, Peng S, Deng X. 2010. Effects of excess boron on growth, gas exchange, and boron status of four orange scion-rootstock combinations. *Journal of Plant Nutrition and Soil Science* 173: 469–476.
- Shorrocks VM. 1997. The occurrence and correction of boron deficiency. *Plant and Soil* 193: 121–148.
- Sparkes IA, Runions J, Kearns A, Hawes C. 2006. Rapid, transient expression of fluorescent fusion proteins in tobacco plants and generation of stably transformed plants. *Nature Protocols* 1: 2019–2025.
- Sutton T, Baumann U, Hayes J, Collins NC, Shi B-J, Schnurbusch T, Hay A, Mayo G, Pallotta M, Tester M *et al.* 2007. Boron-toxicity tolerance in barley arising from efflux transporter amplification. *Science* 318: 1446–1449.
- Takano J, Noguchi K, Yasumori M, Kobayashi M, Gajdos Z, Miwa K, Hayashi H, Yoneyama T, Fujiwara T. 2002. *Arabidopsis* boron transporter for xylem loading. *Nature* 420: 337–340.
- Tao JJ, Chen HW, Ma B, Zhang WK, Chen SY, Zhang JS. 2015. The role of ethylene in plants under salinity stress. *Frontiers in Plant Science* 6: 1059.
- Torun AA, Yazici A, Erdem H, Çakmak İ. 2006. Genotypic variation in tolerance to boron toxicity in 70 durum wheat genotypes. *Turkish Journal of Agriculture and Forestry* 30: 49–58.
- Tu KL, Nghiem LD, Chivas AR. 2010. Boron removal by reverse osmosis membranes in seawater desalination applications. *Separation and Purification Technology* 75: 87–101.
- Vandenbussche F, Vaseva I, Vissenberg K, Van Der Straeten D. 2012. Ethylene in vegetative development: a tale with a riddle. *New Phytologist* 194: 895–909.
- Wang CY, Zhang S, Yu Y, Luo YC, Liu Q, Ju C, Zhang YC, Qu LH, Lucas WJ, Wang X *et al.* 2014. MiR397b regulates both lignin content and seed number in *Arabidopsis* via modulating a laccase involved in lignin biosynthesis. *Plant Biotechnology Journal* 12: 1132–1142.
- Wimmer MA, Abreu I, Bell RW, Bienert MD, Brown PH, Dell B, Fujiwara T, Goldbach HE, Lehto T, Mock HP *et al.* 2020. Boron: an essential element for vascular plants: a comment on Lewis (2019) 'Boron: the essential element for vascular plants that never was'. *New Phytologist* 226: 1232–1237.
- Žárský V, Cvrčková F. 2019. Plant cell morphogenesis: methods and Protocols. In: Walker JM, ed. *Methods in molecular biology*. New York, NY, USA: Humana Press, 34–35.
- Zhang X, Henriques R, Lin SS, Niu QW, Chua NH. 2006. *Agrobacterium*-mediated transformation of *Arabidopsis thaliana* using the floral dip method. *Nature Protocols* 1: 641–646.
- Zhao H, Sun R, Albrecht U, Padmanabhan C, Wang A, Coffey MD, Girke T, Wang Z, Close TJ, Roose M *et al.* 2013. Small RNA profiling reveals phosphorus deficiency as a contributing factor in symptom expression for citrus huanglongbing disease. *Molecular Plant* 6: 301–310.
- Zhong H, Lauchli A. 1993. Changes of cell wall composition and polymer size in primary roots of cotton seedlings under high salinity. *Journal of Experimental Botany* 44: 773–778.

Supporting Information

Additional Supporting Information may be found online in the Supporting Information section at the end of the article.

Fig. S1 Information of the pBI121 vector.

Fig. S2 Alignment of CsiLAC4 and CsiLAC17.

Fig. S3 Topology of CsiLAC4 and CsiLAC17.

Fig. S4 Subcellular localization of CsiLAC4 and CsiLAC17.

Fig. S5 Phylogenetic analysis of CsiLAC17.

Fig. S6 Lignin contents of transgenic *Arabidopsis*.

Fig. S7 Effects of boric acid and NaCl supplements on hypocotyl growth.

Fig. S8 Boric acid excess stimulates early flowering in the CsiLAC4^{OE} lines.

Fig. S9 Effects of boric acid excess on hypocotyl anatomy.

Fig. S10 Effects of boric acid treatments on gene expression in *Arabidopsis*.

Fig. S11 Melting curves of genes tested in this study.

Fig. S12 Effects of boric acid excess on interfascicular fiber thickness in the CsiLAC4^{OE} lines.

Fig. S13 Expression of LACCASE-like family genes in boric acid-treated *Citrus* leaves.

Fig. S14 Effects of boric acid excess on the nutrient accumulation in *Arabidopsis*.

Table S1 Primers for PCR cloning and hybridization.

Table S2 Primers for site-directed mutagenesis.

Table S3 miRNA northern blotting probe.

Table S4 Specific and nested primers for 5'-RACE PCR.

Table S5 Primers for RT-PCR of laccase-like family genes.

Table S6 Boron fractions in *Citrus* leaves treated with different boric acid treatments.

Please note: Wiley Blackwell are not responsible for the content or functionality of any Supporting Information supplied by the authors. Any queries (other than missing material) should be directed to the *New Phytologist* Central Office.



About *New Phytologist*

- *New Phytologist* is an electronic (online-only) journal owned by the New Phytologist Foundation, a **not-for-profit organization** dedicated to the promotion of plant science, facilitating projects from symposia to free access for our Tansley reviews and Tansley insights.
- Regular papers, Letters, Viewpoints, Research reviews, Rapid reports and both Modelling/Theory and Methods papers are encouraged. We are committed to rapid processing, from online submission through to publication 'as ready' via *Early View* – our average time to decision is <26 days. There are **no page or colour charges** and a PDF version will be provided for each article.
- The journal is available online at Wiley Online Library. Visit **www.newphytologist.com** to search the articles and register for table of contents email alerts.
- If you have any questions, do get in touch with Central Office (np-centraloffice@lancaster.ac.uk) or, if it is more convenient, our USA Office (np-usaoffice@lancaster.ac.uk)
- For submission instructions, subscription and all the latest information visit **www.newphytologist.com**